Department of Communications
Communications Research Centre

Ministère des Communications
Centre de recherches sur les communications

Title:

Further Investigation of Code Division Multiple Access Techniques

Authors: **C.D.Amours and A.Yongaçoglu**
University of Ottawa
Department of Electrical Engineering

Date: **March 1993**

DOC Contractor Report: CRC-CR-93-003
DSS Contract No.: CRC36001-2-3617

Scientific Authority: Michael Moher
Classification: Unclassified

Contents

List of Figures

1 Introduction

The capacity of a CDMA system is a function of the bit error performance of individual users. Therefore it is important to optimize the individual links before proceeding to system level analysis. The concern about employing DS-CDMA in frequency-selective Rayleigh fading channels is that the performance will be poor, thus leading to inefficient channel use. However, the nature of DS-CDMA signals along with that of the channel allows the receiver to resolve the signal into different diversity paths by employing a RAKE receiver. Such a receiver was investigated in [1] for different detection and coding schemes. The results suggested that higher capacities can be obtained by employing a pilot symbol-assisted coherent detection scheme rather than a differential detection scheme.

Pilot symbol-assisted modulation (PSAM) is discussed in [2,3]. The system used in [1] employs the low pass filtering approach of [3] rather than the optimum Weiner filtering approach which is analyzed in [2]. This suggests that the results obtained in [1] can be improved by modifying the receiver structure to ressemble the one discussed in [2].

This report is organized in seven sections. Section 2 discusses pilot symbol-assisted modulation in both frequency-nonselective and frequency-selective fading channels. Section 3 attempts to optimize the pilot symbol insertion rate for different fading bandwidth to signal bandwidth ratios (B_dT_s). Section 4 discusses the effect of self noise generated between different components of a frequency-selective faded signal and how this is accomplished in the simulation package. Section 5 investigates the effect of interleaver span on the bit error performance of PSAM. Section 6 investigates the effect of the increased symbol rate due to the insertion of pilot symbols on the processing gain of a DS-CDMA system. Section 7 investigates the effect of PN sequence length, and Section 8 presents all conclusions drawn from this study.

2 Pilot Symbol-Assisted Modulation

In a pilot symbol-assisted modulation scheme, known symbols are inserted periodically into the data sequence prior to pulse shaping. With this approach, the receiver processes the signal with a matched filter as illustrated in Figure 1. The symbol-spaced samples of the matched filter output are given by

$$r(k) = u(k)b(k) + n(k) \tag{1}$$

where $b(k)$ is the kth symbol normalized to unit variance, $u(k)$ is the kth symbol complex gain, and $n(k)$ are white Gaussian noise samples with unit variance. This assumes slow fading, that is, there is negligible change in the channel over the duration of a pulse shape, and that the transmitter and receiver filters are designed for no ISI at the sample points. For a Rayleigh fading channel, the channel gain has variance

$$\sigma_u^2 = \frac{1}{2}E\left(|u|^2\right) = \frac{(M-1)}{M}\frac{E_s}{N_o} \tag{2}$$

assuming one pilot symbol per frame of M transmitted symbols and equal power in the pilot symbols and the data symbols.

The reference branch of Figure 1 extracts the pilot samples and uses them to estimate the channel, both its phase and gain. A delay matching that of the channel estimation process is introduced into the symbol stream to maintain the correct correspondence between the channel estimates and detected symbols. To explain the channel estimation process consider, without a loss of generality, frame 0, $(k = 0, ..., M-1)$. Assume b_0 is a pilot symbol and define the length K column vector p as the set of pilot symbols $r(iM)$ where $(-\lfloor\frac{K}{2}\rfloor \leq i \leq \lfloor\frac{K}{2}\rfloor)$. Also define R as the autocorrelation function of the pilot samples

$$R = \frac{1}{2}E[pp^H] \tag{3}$$

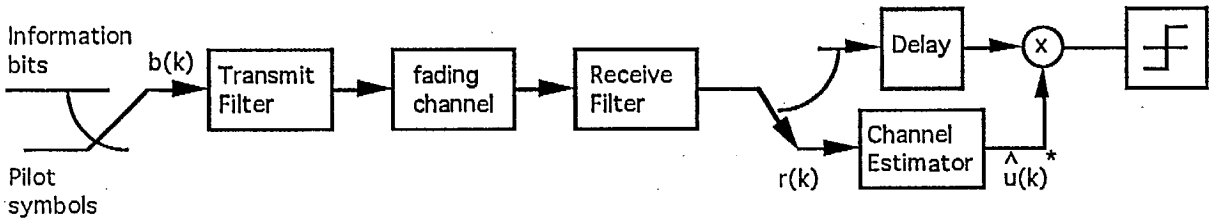

Figure 1: Block diagram of a pilot symbol-assisted communication system.

and $w(k)$ as the crosscorrelation of the channel gain within frame 0 with the pilot samples p.

$$w(k) = \frac{1}{2}E[u(k)^* p] \qquad \text{for } k = 1, ..., M-1 \tag{4}$$

As shown in [2], the optimum estimator for the channel at time k, using the K nearest pilot symbols is

$$\hat{u}(k) = \left(R^{-1}w(k)\right)^H p \tag{5}$$

Note that the optimal estimator is a function of both the channel and the operating signal to noise ratio. In practice, one would typically use a fixed estimator derived from (5) at the assumed operating point, that is,

$$\hat{u}(k) = h(k)^H p \tag{6}$$

Note that the estimator $h(k)$ depends on the position k within the frame. As demonstrated in [2], suboptimum estimators derived in this manner result in only

a marginal loss in performance over a wide range of operating conditions. The same is not true of the low pass filtering approach suggested in [3].

The resulting channel estimate can equivalently be used to either scale the decision boundaries or scale the received data. From [2], the expected uncoded bit error rate performance of this modulation/detection scheme for a bit in position k of a frame is given by

$$P_b(k) = \frac{1}{2}\left(1 - \sqrt{Re[\rho(k)]^2/(1 - Im[\rho(k)])^2}\right) \tag{7}$$

where

$$\rho(k) = \frac{w(k)^H h(k)}{\sqrt{\sigma_u^2 h(k)^H R h(k)}} \tag{8}$$

and $h(k)$ is the channel estimator described by (6) (either optimum or suboptimum). The average bit error rate must be obtained by averaging over all bit positions k, $k = 1, ..., M-1$ within a frame. To evaluate the above, one can make the common assumption of a U-shaped fading spectrum of isotropic scattering corresponding to the autocorrelation function [4]

$$R^u(\tau) = \sigma_u^2 J_o(2\pi f_D \tau) \tag{9}$$

for the fading process where f_D is the Doppler frequency and J_o is the Bessel function. With this assumption, the ijth element of the autocorrelation function R is given by

$$R_{ij} = \sigma_u^2 J_o(2\pi f_D T M|i-j|) + \delta_{ij} \tag{10}$$

where T is the symbol period and δ_{ij} is the Kronecker delta. The ith element of the crosscorrelation vector $w(k)$ is similarly given by

$$(w(k))_i = \sigma_u^2 J_o(2\pi f_D T|M(i - \lfloor K/2 \rfloor - 1) + k|) \tag{11}$$

These results can be extended to the frequency-selective case when a DS-SS system is used with pilot symbols inserted at the transmitter and a RAKE receiver as depicted in Figure 2. The action of the despreading makes the signal on each branch of the RAKE receiver appear as the output of a Rayleigh flat-fading channel so the above analysis applies to each branch of the RAKE receiver. Furthermore, if one assumes that the contents of each branch has faded independently, and has the same average power, then in the case of L taps, one has an Lth order diversity system. The results of [2], given above, and the analysis of diversity systems discussed in [5] imply that the expected bit error rate performance is given by

$$P = (P_b)^L \sum_{k=0}^{L-1} \binom{L-1+k}{k} (1 - P_b)^k \tag{12}$$

where P_b is the average bit error rate of a Rayleigh flat fading channel derived from (7) at a nominal E_s/N_o of γ dB, and P is the average bit error rate of an Lth order diversity system with a total $E_s/N_o = \gamma + 10\log(L)$ dB.

3 Optimization of Pilot Symbol Insertion Rate

By inserting pilot symbols into the information stream, some of the signal power is removed from the information and given to the pilot symbols. As the pilot symbol insertion rate is increased, the channel estimation process becomes more reliable, while the information, which now contains less power, becomes less reliable. Thus, there should exist a pilot symbol insertion rate that gives the best overall bit error rate for a given fading rate.

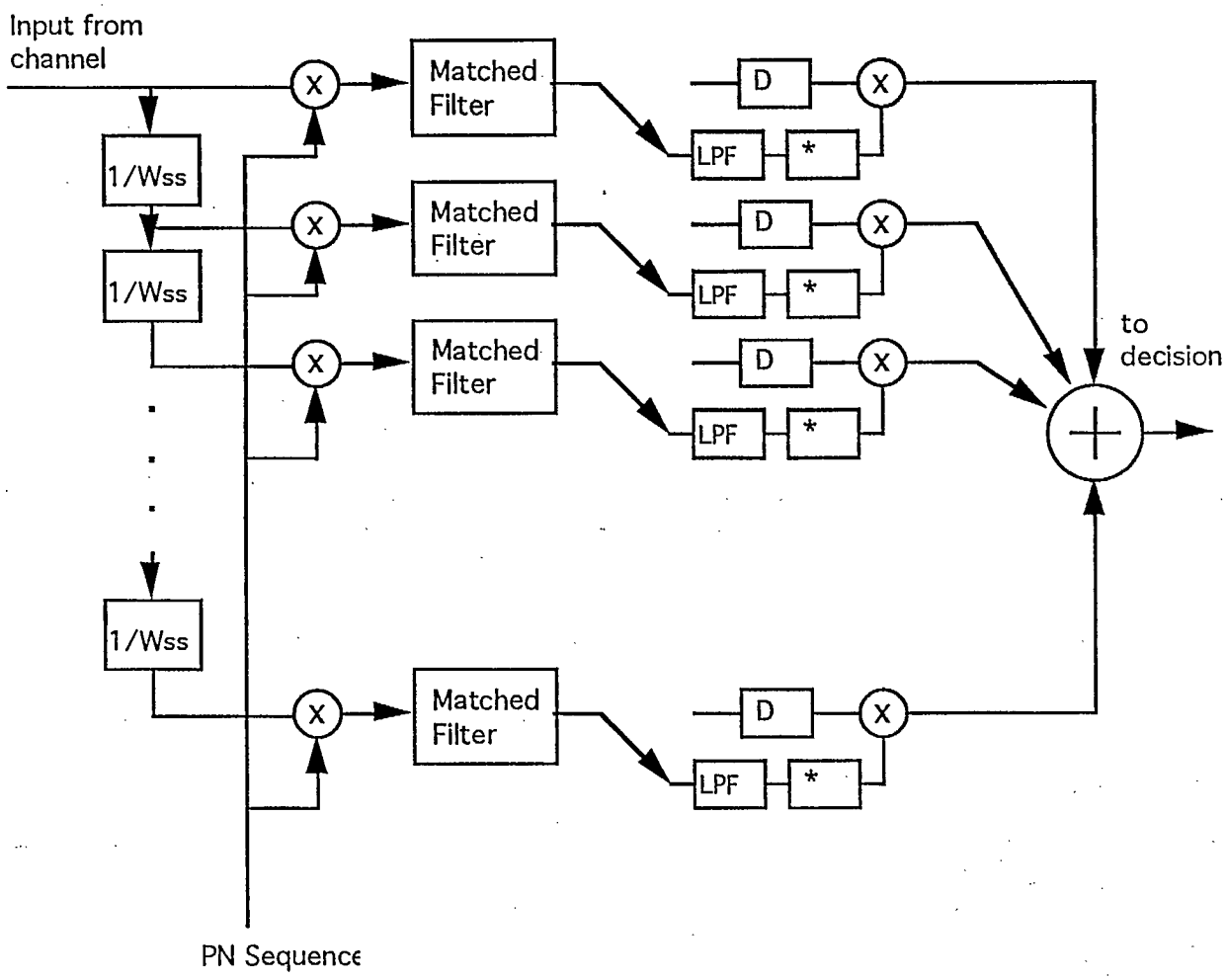

Figure 2: Pilot symbol-assisted RAKE receiver.

Pilot symbol-assisted modulation divides the information into a number of frames of size M. Each frame is made up of one pilot symbol followed by $M-1$ information symbols. As seen in [2], the bit error rate of a PSAM system is quite insensitive to the pilot symbol insertion rate. Frame sizes of 5, 11, and 21 are considered in this section. All estimation filters are designed to be optimum at $E_s/N_o = 10$dB. At any given instant, the estimation filter sees K different pilot symbols. To reduce complexity of these filters, K is selected to be 5.

For all simulations presented in this report, the same system conditions as in [1] are assumed. In other words, the uncoded information rate is 10 kbps, the fading rate is 125 Hz, and the spread bandwidth is 1.28 MHz.

Figure 3 demonstrates the bit error performance of a PSAM system in a frequency-nonselective fading channel with a fading rate of 125 Hz (assuming 10 kbps, then $B_dT_s = 0.0125$). Theoretical results are given for estimation filters designed to be optimum at $E_b/N_o = 10$ dB. Note that at high E_b/N_o the curves differ greatly from the theoretical results. The reason for this deviation will be explained at the end of this section. Despite the deviation between theory and analysis, it is clear from both that $M = 5$ provides the best results.

Employing PSAM along with a RAKE receiver for a frequency-selective fading channel with the same fading rate, we should expect to find that the same frame size will provide the same results. Figure 4 shows the bit error rate performance of PSAM when 5 distinct signal components are present and received by the RAKE receiver. Once again, the simulated curves deviate from the theoretical curves at high E_b/N_o. Also, the theoretical curves (from eq. 12) do not take the self-noise between the different multipath components into account while the simulated curves do. Once again, both simulated and theoretical curves show that a frame size of $M = 5$ provides the best results for this fading rate.

Suppose that the information rate is now doubled (i.e. rate 1/2 coding is employed, $B_dT_s = 0.00625$). Clearly, it may be possible to decrease the insertion rate without sacrificing bit error rate performance. Figure 5 shows the raw bit error performance of PSAM with $M = 5$, 11, and 21 in a frequency-nonselective fading channel with $B_dT_s = 0.00625$. Once again, the simulated curves deviate from the analytical curves due to the nature of the fading filter used in the simulations,

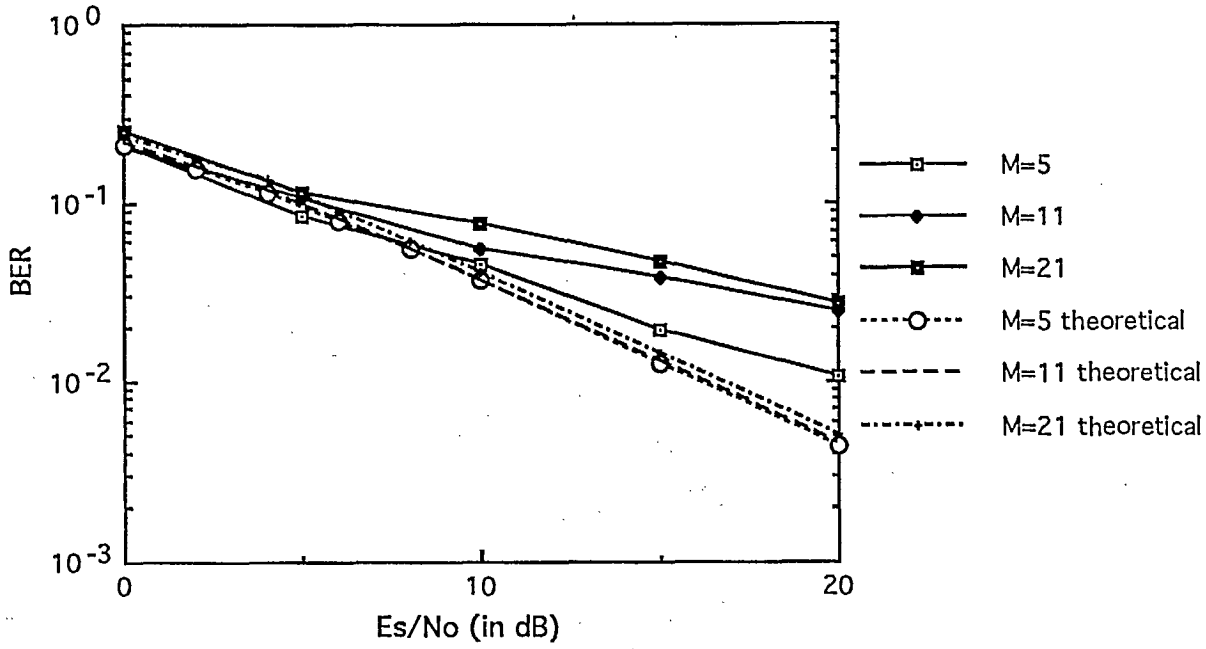

Figure 3: Performance of PSAM for $M = 5$, 11 and 21 in frequency-nonselective fading ($B_d T_s = 0.0125$).

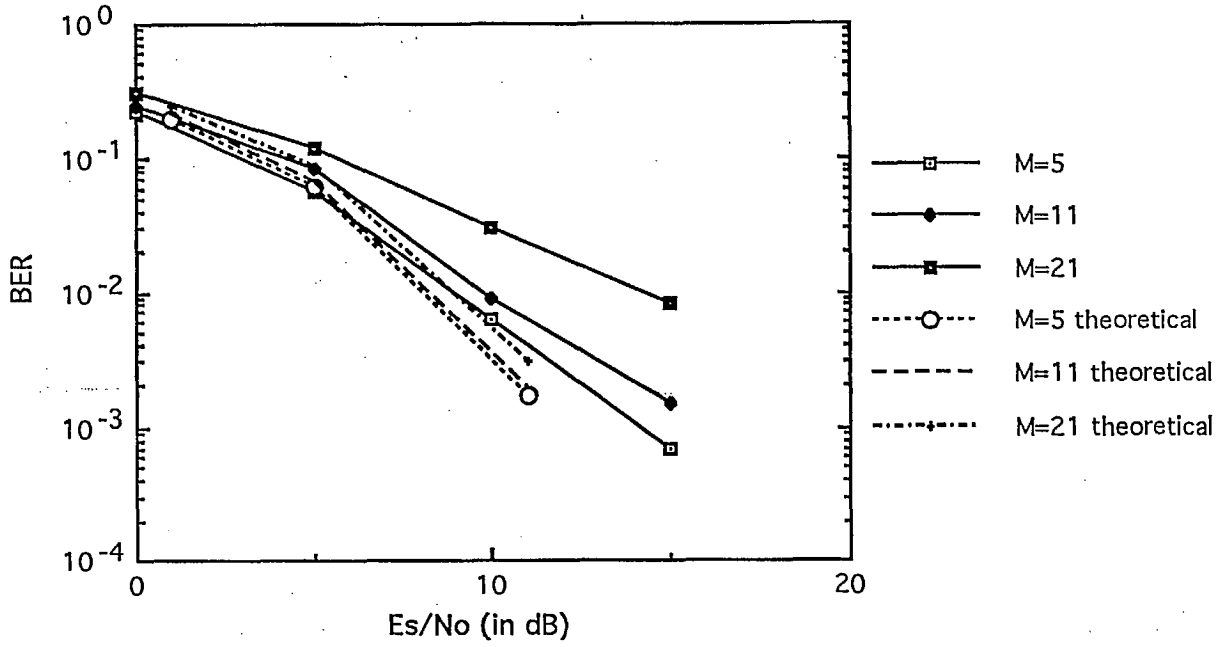

Figure 4: Performance of PSAM for $M = 5$, 11 and 21 in frequency-selective fading ($B_d T_s = 0.0125$).

which deviates from an ideal filter used in the analysis. In this figure, we can see that $M = 11$ provides the best results in the simulated curves for low E_b/N_o. At higher E_b/N_o $M = 5$ becomes the best frame size. The analytical curves agree with this, however the crossover point is at a much higher E_b/N_o than for the simulated curves. This crossover is due to the tradeoff between pilot and information power. At low E_s/N_o, allocating too much power to the pilot causes the information to be unreliable, yet at high E_s/N_o, where the information is reliable, we can allocate more power to the pilot thus making the channel estimation process more reliable. Also, the deviation from theoretical results tends to indicate that an error floor is present. This error floor may be dependent on the frame size as well as the fading rate. This possibility will be discussed at the end of this section. Since it is our goal to use this system with rate 1/2 coding, we desire a system which performs well at low E_s/N_o. Therefore it would be wise to employ $M = 11$ when using rate 1/2 convolutional coding.

Figure 6 shows the bit error rate performance of a DS-CDMA PSAM RAKE received signal made up of 5 distinct components with a fading rate $B_dT_s = 0.00625$. The results of Figure 6 agree with those of Figure 5 in that the best system at low E_b/N_o is that which employs a frame size of 11.

Suppose we now wish to employ rate 1/4 convolutional coding in our spread spectrum system. Thus $B_dT_s = 0.003125$. Figure 7 shows the raw bit error performance of PSAM in frequency-nonselective Rayleigh fading for $M = 5$, 11, and 21. At low E_b/N_o, there is little difference between the performances of the three PSAM systems. However, it appears that $M = 11$ provides the best results in this case. From the theoretical curves, $M = 11$ and $M = 21$ seem to perform equally well with $M = 5$ performing worse. In the simulated case, it appears that $M = 21$ performs worse.

Figure 8 shows the bit error performance of a DS-CDMA PSAM system using a RAKE receiver when the channel is frequency-selective with 5 resolvable components. Again, we see that the theoretical performance of $M = 11$ and $M = 21$ are similar, however, the simulated system performs best when $M = 11$. These results agree with the results found in Figure 7.

If such a system were to employ rate 1/8 convolutional coding, then $B_dT_s =$

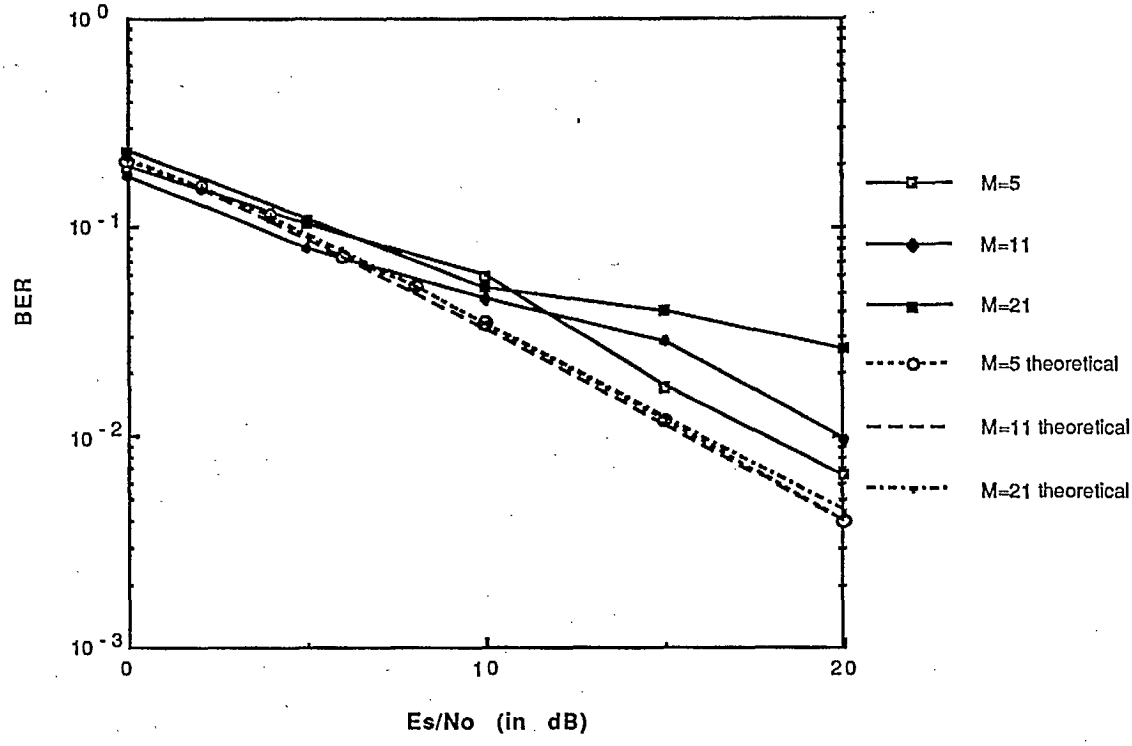

Figure 5: Performance of PSAM for $M = 5$, 11 and 21 in frequency-nonselective fading ($B_d T_s = 0.00625$).

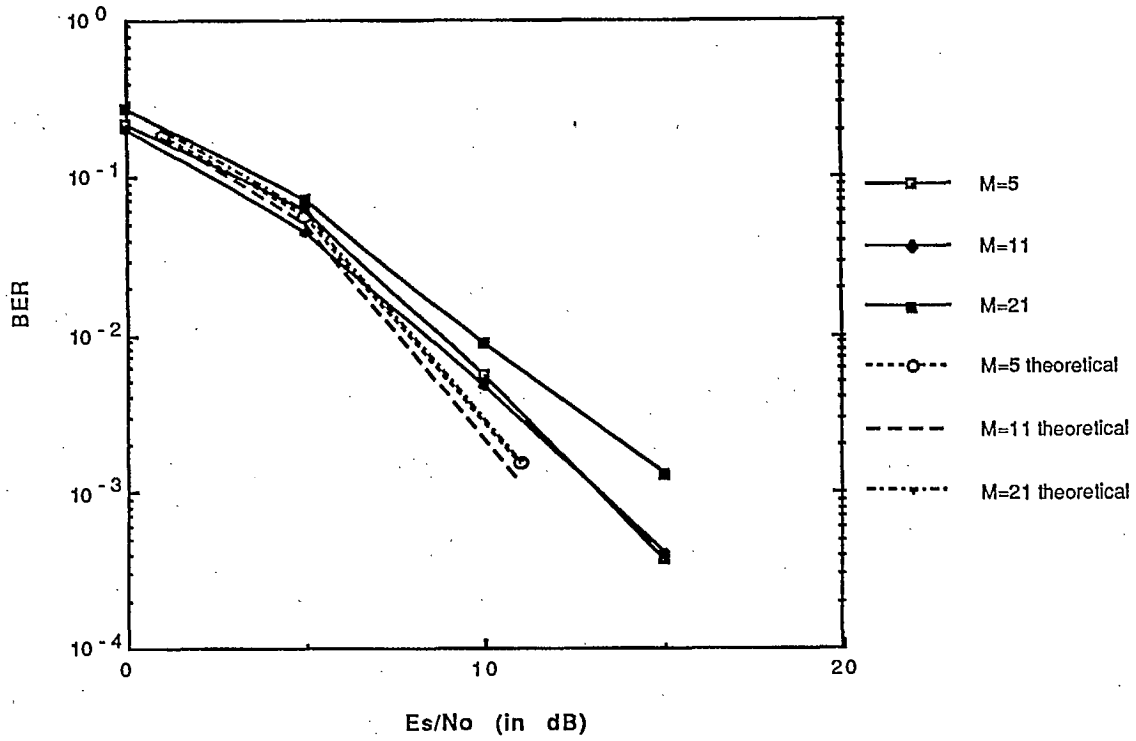

Figure 6: Performance of PSAM for $M = 5$, 11 and 21 in frequency-selective fading ($B_d T_s = 0.00625$).

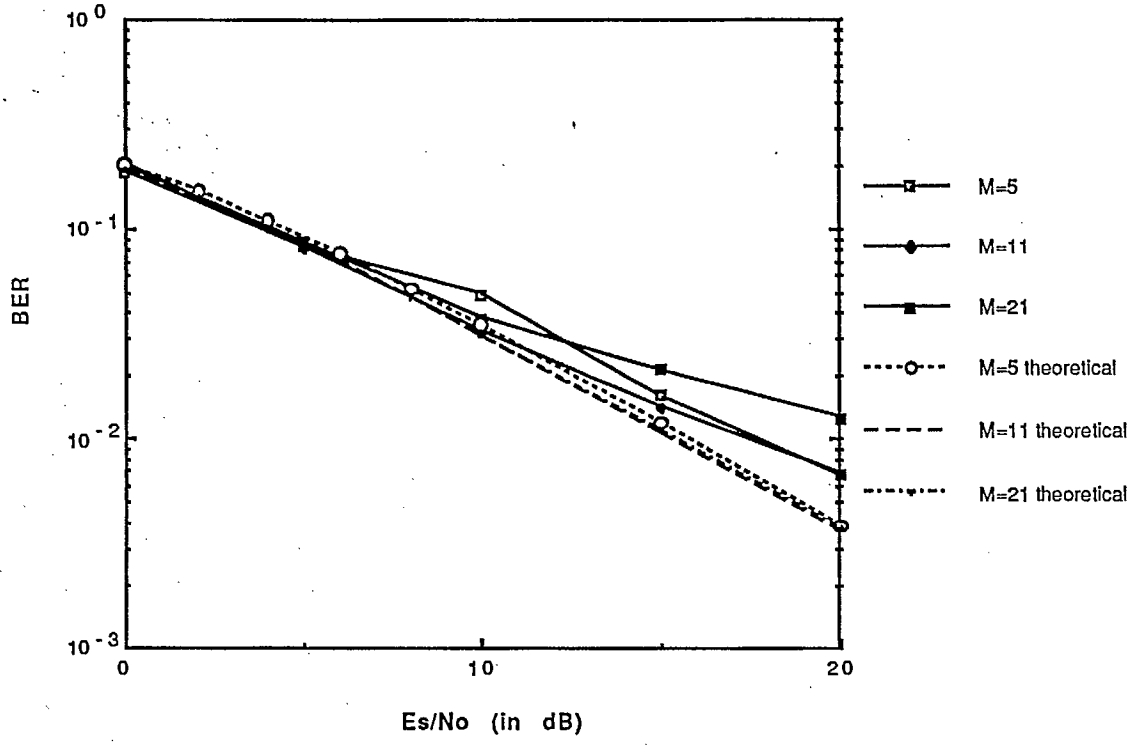

Figure 7: Performance of PSAM for $M = 5$, 11 and 21 in frequency-nonselective fading ($B_d T_s = 0.003125$).

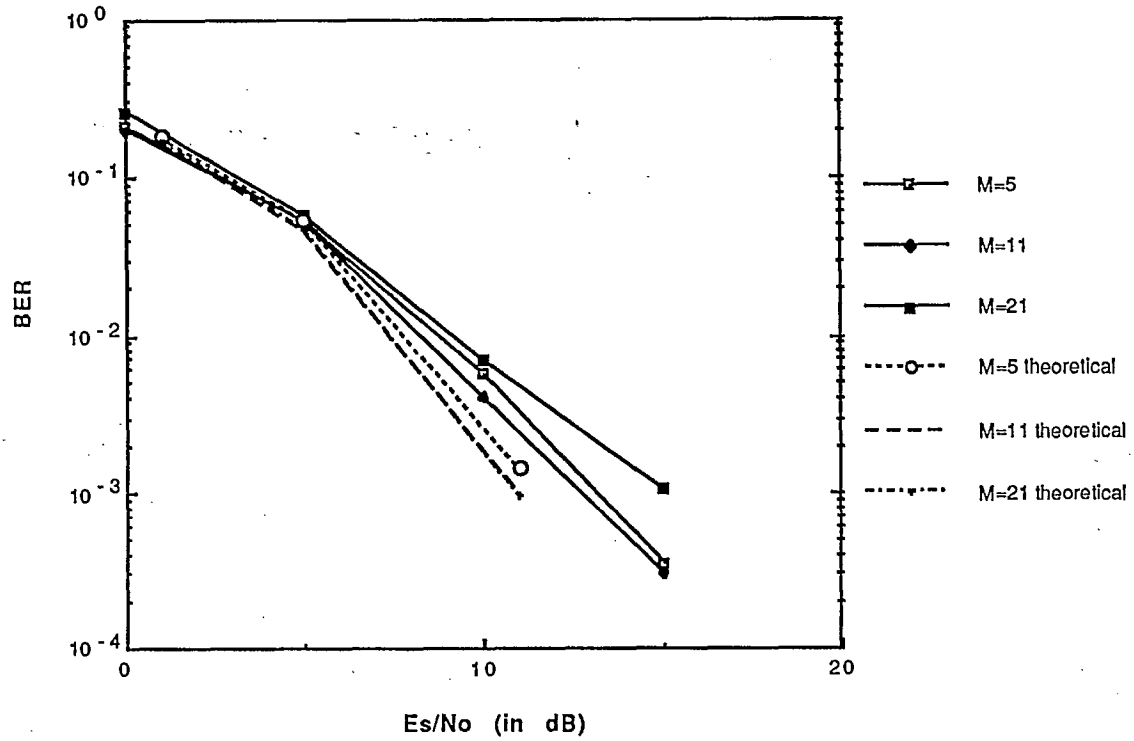

Figure 8: Performance of PSAM for $M = 5$, 11 and 21 in frequency-selective fading ($B_d T_s = 0.003125$).

0.0015625. Figure 9 demonstrates the predecoding symbol error rate for PSAM in frequency-nonselective Rayleigh fading for $B_dT_s = 0.0015625$. In this figure, the simulated curves for $M = 11$ and $M = 21$ are quite similar. The theoretical values for the bit error performance suggests that $M = 21$ performs slightly better than $M = 11$ when $B_dT_s = 0.015625$.

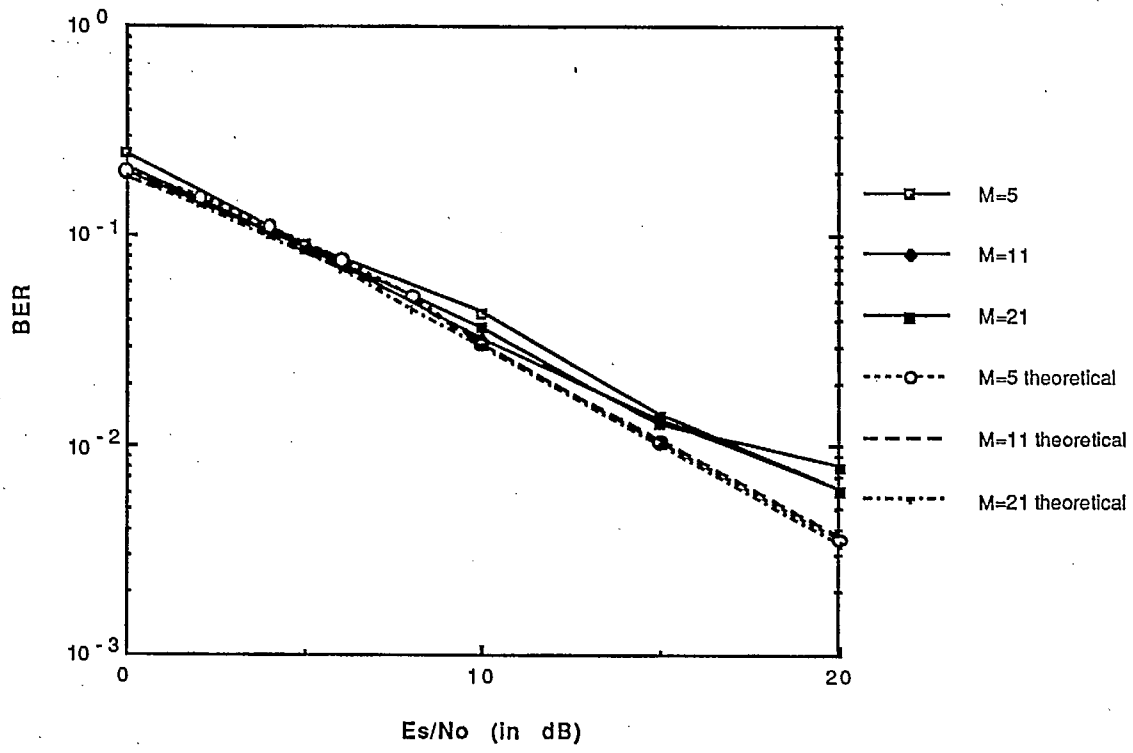

Figure 9: Performance of PSAM for $M = 5$, 11 and 21 in frequency-nonselective fading ($B_dT_s = 0.0015625$).

For a frequency-selective channel, which produces 5 distinct signal components when received by a RAKE receiver, Figure 10 demonstrates the bit error performance of PSAM for the three different frame lengths. From this figure, we can

see that $M = 21$ provides the best results when E_s/N_o is low. Since we wish to employ this system with rate 1/8 convolutional coding, this frame size will provide the best results.

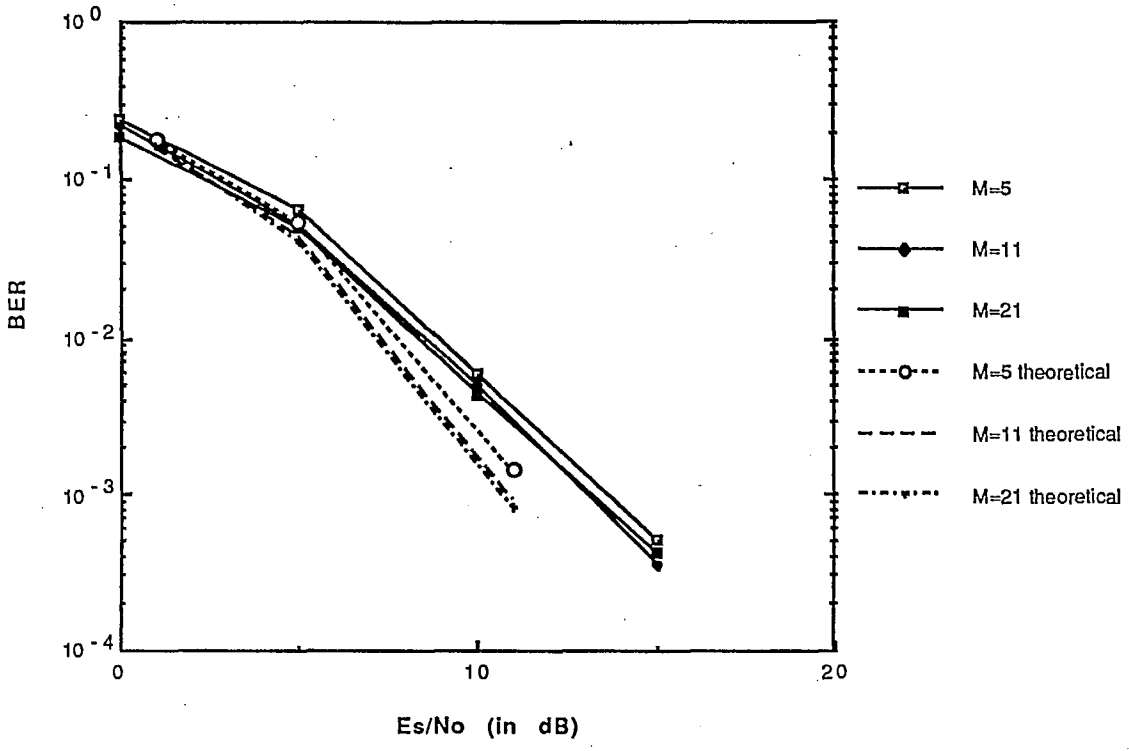

Figure 10: Performance of PSAM for $M = 5$, 11 and 21 in frequency-selective fading ($B_dT_s = 0.0015625$).

In this section, we observed the performance of PSAM in both frequency-nonselective fading and in frequency-selective fading using direct-sequence spread spectrum and RAKE reception. The simulated performance of these systems were compared to the theoretical performances derived in Section 2 and in [2]. Although the simulations and the theory generally agreed on the best choice for the frame length, M,

the simulated performance curves tended to deviate from theory at high E_s/N_o. Simulations performed without AWGN noise for different fading rates indicate that a significant irreducible error floor; which is dependent on both the fading rate and the frame size, is present. However, simulations performed without noise or fading yield error free transmissions. This indicates that perhaps the analysis ignores some aspect which causes this error floor or perhaps the error floors in the simulations are due to the method used for implementing the fading process in the simulations. The fading process is implemented by filtering a Gaussian process using a FIR filter which has approximately a constant frequency response in the passband. The analysis assumes that the fading process has a U-shaped spectrum and thus an estimation filter designed using the analysis of [2] is not exactly matched to the channel used in the simulations.

In conclusion, from the results presented in this section, better pilot symbol insertion rates are presented compared to [1], thus providing us with the potential to improve the results found in [1].

4 Effect of Self-Noise due to Multipath Components

In [6], Viterbi shows that the equivalent signal energy to noise spectral density ratio for an asynchronous multiple user spread spectrum system is given by

$$\frac{E_b}{N_{o\ eq}} = \frac{E_b/N_o}{1+(U-1)(1/B_c)(E_b/N_o)} \tag{13}$$

where U is the number of simultaneous users, B_c is the bandwidth expansion factor and is equal to R_c/R_s (R_c is the chip rate and R_s is the symbol rate), E_b/N_o is the single user signal energy to noise spectral density ratio, and $N_{o\ eq}$ is the equivalent noise spectral density which includes the multiple access interference (i.e., self noise).

In a frequency-selective fading channel, signal components which are delayed by more than one chip time relative to one another behave as multiple users. Thus each component received by the RAKE receiver provides some interference to each other component. Thus the equivalent signal energy to spectral noise density ratio, $\gamma_{i\ eq}$ of the ith tap of the RAKE receiver is given by

$$\gamma_{i\ eq} = \frac{\gamma_i}{1 + \sum_{j \neq i} (1/B_c)(\gamma_i)} \tag{14}$$

The denominator of this expression represents the increase in equivalent white noise power. For the simulations presented in [1] and this report, this increase in noise power is calculated for each received component, and the white noise is increased accordingly.

5 Effect of Interleaving Span on Performance of Coded PSAM

In Rayleigh fading channels, deep fades can cause long error bursts. When convolutional encoding is used, this can cause an unacceptable bit error performance without the use of interleaving. By interleaving and de-interleaving, the positions of errors within an information stream are randomized, thus maximizing the gain provided by convolutional decoding. However, the span of the interleaving process must be much larger than the duration of the error bursts which are present. In this section, different interleaver spans are considered for convolutionally encoded PSAM signals. For the simulations presented in this section, the same estimation filters designed for Section 3 are used.

Figure 11 presents the bit error performance of PSAM in frequency-nonselective Rayleigh fading using rate 1/2 constraint length 7 convolutional coding. For this simulation, $M = 11$ which was the frame length which provided the best raw bit error performance in Section 3 for $B_d T_s = 0.00625$. From this figure, we can see that the effect of increasing the interleaver span is negligible when E_b/N_o is

small. However, at high E_b/N_o, 60 msec interleaving appears to provide some improvement in the bit error performance of rate 1/2 convolutionally encoded PSAM.

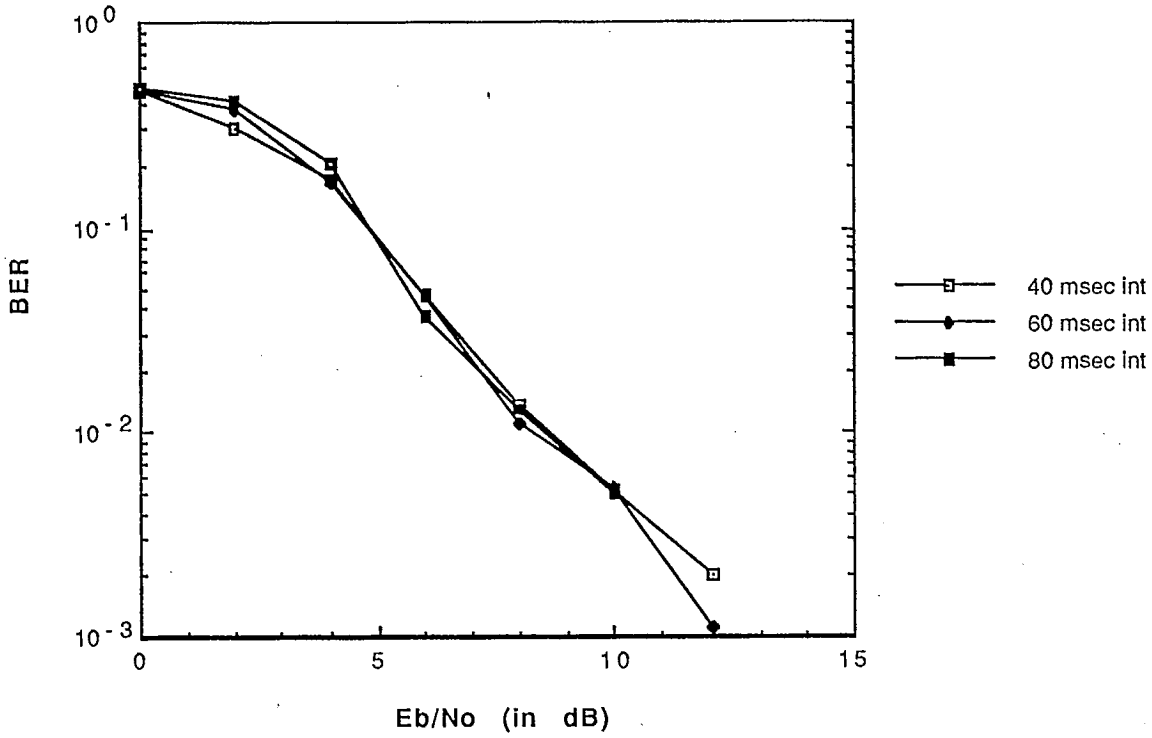

Figure 11: Performance of rate 1/2 convolutionally encoded PSAM in frequency-nonselective Rayleigh fading with different interleaving spans.

The bit error performance of rate 1/4 convolutionally encoded PSAM ($M = 11$) in frequency-nonselective Rayleigh fading is shown in Figure 12. Due to memory constraints on the software used, a maximum interleaver span of only 50 msec is possible when rate 1/4 coding is used. We can see that the 50 msec interleaver provides some improvement over the 40 msec interleaver at high E_b/N_o. At the

high E_b/No, the raw bit error rate must be dominated by errors due to deep fades, and the slightly higher interleaver span better randomizes these burst errors.

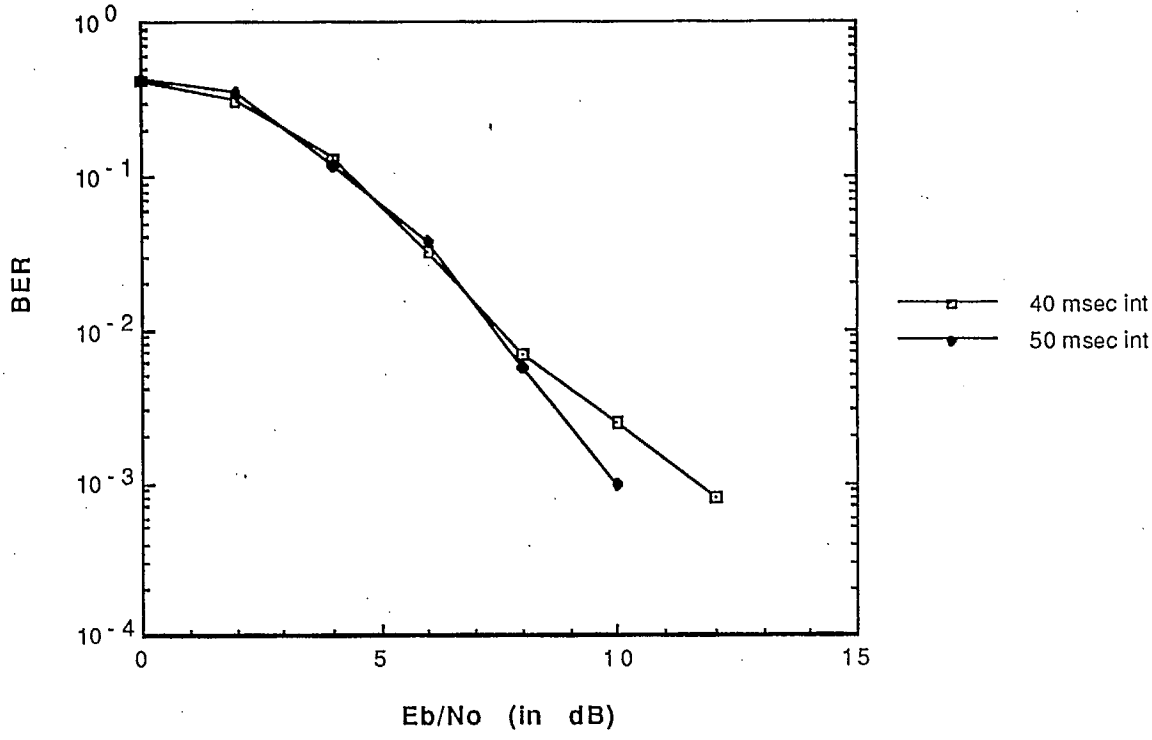

Figure 12: Performance of rate 1/4 convolutionally encoded PSAM in frequency-nonselective Rayleigh fading with different interleaving spans.

Unfortunately, due to memory constraints, rate 1/8 convolutional coding could not be performed with large interleaver spans. It was seen in Figure 11 that the 40 msec interleaving was not sufficient in randomizing the channel errors for the rate 1/2 convolutional code, and that 60 msec interleaving provides improvements over 40 msec interleaving at high E_b/N_o. In Figure 12, we see that perhaps an interleaver span of 50 msec is needed to fully randomize the channel errors for the

rate 1/4 convolutional coding case.

6 Effect of Pilot Symbols on Processing Gain of DS-CDMA System

By inserting pilot symbols into the information stream, the channel symbol rate is increased. Thus the spreading factor of the DS-CDMA signal is decreased compared to a system which does not employ pilot symbols. However, if we compare two spread spectrum systems, each employing the same bit rate and the same spread bandwidth, but only one employing pilot symbols, we can show that these two systems have an equivalent processing gain.

Using eq. (13), the equivalent signal energy to noise spectral density ratio for the spread spectrum system not employing pilot symbols is given by

$$\frac{E_b}{N_{o\ eq}} = \frac{E_b/N_o}{1 + (U-1)(B/W_{ss})(E_b/N_o)} \tag{15}$$

where E_b is the energy per bit, B is the bandwidth of the unspread signal, and W_{ss} is the bandwidth of the spread signal (also referred to as the spread bandwidth).

For the spread spectrum system using pilot symbols, the equivalent signal energy to noise spectral density ratio is given by

$$\frac{E_s}{N_{o\ eq}} = \frac{E_s/N_o}{1 + (U-1)(B_p/W_{ss})(E_s/N_o)} \tag{16}$$

where E_s is the energy of a channel symbol (which may be an information symbol or a pilot symbol) and B_p is the bandwidth of the information signal with the inclusion of pilot symbols.

If the PSAM transmission is divided into frames of length M, where there are $M-1$ information bits and one pilot symbol, then clearly $B_p = \frac{M}{M-1}B$. Also, assuming that both systems are transmitting at the same power, $E_s = \frac{M-1}{M}E_b$. Placing these expressions into eq. (16). the following is obtained

$$\frac{E_s}{N_{o\ eq}} = \frac{\frac{M-1}{M}E_b/N_o}{1+(U-1)(\frac{M}{M-1}B/W_{ss})(\frac{M-1}{M}E_b/N_o)} \tag{17}$$

which becomes

$$\frac{E_s}{N_{o\ eq}} = \frac{\frac{M-1}{M}E_b/N_o}{1+(U-1)(B/W_{ss})(E_b/N_o)} = \frac{M-1}{M}\frac{E_b}{N_{o\ eq}} \tag{18}$$

However, $E_s = \frac{M-1}{M}E_b$. The only loss in symbol energy is caused by the loss of symbol energy due to the increased symbol rate, which is expected. In other words, the equivalent noise spectral densities of the two spread spectrum systems are the same despite the increased bandwidth of the pilot symbol-assisted system. Since there is no other loss, these two systems must have the same processing gain. This result can be extended to include systems which include error control coding as shown in [6].

7 Selecting the Period of the Spreading Code

In the uncoded case, the total spreading of l is achieved by using a PN sequence. In the case with a rate r code, coding provides a spreading of $1/r$. Hence the spreading to be achieved by the PN sequence is only $l \cdot r$. In other words, the number of chips per channel symbol is $N_c = l \cdot r$.

In the uncoded case, we assumed that the period p of the PN sequence is equal to l. As discussed in several published works, choosing $p = l$ for the uncoded case is

the appropriate and frequently used approach for CDMA applications [7-10]. For some non-CDMA applications, choosing $p >> l$ can be beneficial [11,12] and in these cases the PN sequence is referred to as the "long code" (as opposed to the short code where $l = p$).

Another issue discussed in the literature is the tradeoff between the processing gain and the coding gain [13]. Since in this report we have studied the performance of certain codes and found when they give the best performance (e.g. constraint length 7 rate 1/8 code for the pilot-symbol assisted system), our aim is to find what should be the period of the sequence to provide the rest of the spreading.

For the system which uses FEC coding, the two main options are:

(i) to use a sequence with period $p = l = N_c/r$ (i.e., one period per information bit);

(ii) to use a sequence with period $p = l \cdot r = N_c$ (i.e., one period per channel bit).

In both cases it is assumed that the number of chips per symbol is the same, i.e. $N_c = l \cdot r$.

The PN code length will impact the following aspects.

(i) Total number of distinct codes that can be employed.

(ii) Synchronization properties.

(iii) Correlation properties.

There are also other issues such as security (which favors codes with longer period), but these are of secondary importance in the code selection for CDMA. Let us now briefly discuss each of the three properties listed above.

(i) Total Number of Codes

The total number of distinct codes, i.e., the set size increases with the period. For example when the period of the Gold code is $p = 2^m - 1$, the set size is $2^m + 1$. Hence from the set size point of view, choosing $p = N_c/r$ is clearly superior to

$p = N_c$.

(i) Synchronization

In general, the PN code synchronization time increases as the period increases. For example, if the conventional single dwell acquisition technique is used, the correlation is performed with an integration time of pT_c, the duration of one period of the sequence. The maximum number of correlations to be performed before acquisition occurs is p, implying a maximum correlation time of p^2T_c seconds. The average acquisition time is then $p^2T_c/2$ seconds [14]. Hence from the synchronization point of view, generally shorter PN sequences are preferable. However, in a RAKE receiver, it is assumed that there will be l branches. Therefore, as long as $p \leq l$, the coarse acquisition may be easily achieved irrespective of p.

Correlation Properties

The sequence length is important in determining the correlation properties, which in turn determine the error probability performance of a CDMA system.

Let us momentarily consider a coherent BPSK system in an AWGN channel. The bit error probability of signal j in the presence of k simultaneous interferers is [15]

$$P_b = Q(\sqrt{\mathrm{SNR}_j(k)})$$

where

$$\mathrm{SNR}_j(k) = [\frac{N_o}{2E_b} + \frac{R_j(k)}{6N_c^3}]^{-1}$$

and

$$R_j(k) = \sum_{i=1, i\neq j}^{k} r_{i,j}$$

The term $6N_c^3/R_j(k)$ is the signal to multiple access interference ratio. The term $r_{i,j}$ represents the average interference (or correlation) parameter for a PN sequence

i and j and is given by [16]

$$r_{i,j} = 2N_c^2 + 4\sum_{l=1}^{N_c-1} C_i(l)C_j(l) + \sum_{l=1-N_c}^{N_c-1} C_i(l)C_j(l+1)$$

where $C_u(l)$ is the discrete aperiodic autocorrelation function for the PN sequence u of length N_c.

$$C_u(l) = \begin{cases} \sum_{n=0}^{N_c-1-l} u_n u_{n+1} & \text{for } 0 \le l \le N_c - 1 \\ \sum_{n=0}^{N_c-1-l} u_{n-l} u_n & \text{for } 1 - N_c \le l < 0 \\ 0 & |l| \ge N_c \end{cases}$$

In [17], Sarwate et al investigated the partial correlation effects in DS-SSMA systems. They considered the cases when:

(i) $N_c = p$, and

(ii) N_c is a divisor of p.

When $N_c = p$, the average correlation parameter is $r_{i,j} = 2N_c^2$. Note that this is the average value, the actual values may vary significantly from this average value as a function of the phases of the sequences and the particular class of sequence selected (e.g. Gold, m-sequence etc). By proper selection of the phases, significant reduction in the correlation parameter is possible [17].

For the case when N_c is a divisor of p, two constructions which have the average correlation parameter as $2N_c^2$ have been proposed [17]. However, in this case the improvement by proper phase selection may not be as significant.

8 Conclusions

The study of DS-CDMA in Rayleigh fading channels [1] has left a few questions unanswered. In that study, PSAM provided the best bit error performance, and

thus the higher overall system capacity. However, no attempt was made to optimize the pilot symbol insertion rate. In this report, we tried to answer this question and can draw the following conclusions:

1) Pilot symbol-assisted modulation's bit error performance is somewhat insensitive to the pilot symbol insertion rate so long as the channel is sampled at the Nyquist rate or higher.

2) The theoretical and simulated performances of PSAM indicate that the optimum frames sizes are about $M = 5$, 11, 11, and 21 when $B_d T_s = 0.0125$, 0.00625, 0.003125, and 0.0015625 respectively.

3) Simulations indicate that 40 msec interleaving may not be sufficient when rate 1/2 constraint length 7 convolutional coding is used with PSAM. 60 msec interleaving provides better bit error performance at high E_b/N_o. When rate 1/4 constraint length 7 convolutional coding is used, increasing the interleaving span to 50 msec provides a better bit error performance.

4) Analysis based on Viterbi's argument [6] shows that spread spectrum systems which employ PSAM have the same processing gain as spread spectrum systems which do not employ pilot symbols. This is because the addition of pilot symbols accomplishes some of the spectral spreading.

5) From the discussion presented above, the following conclusion can be drawn. Set size considerations favor sequences with longer periods. This is particularly true for low rate codes such as rate 1/8. However, if the selected sequence length supports a sufficiently large number of users, then it may be easier to achieve lower partial correlation with a sequence of length $N_c = p$ than with a sequence where N_c is a divisor of p. An added advantage of this choice might be improved synchronization properties.

Bibliography

[1] C. D'Amours, J. Wang, A. Yongaçoğlu, "To Analyze Through Simulation Coding, Modulation and Detection Strategies for Code Division Multiple Access Sys-

tems", DSS Contract No. CRC36001-1-3586, March 31, 1992.

[2] J.K. Cavers, "An Analysis of Pilot Symbol Assisted Modulation for Rayleigh Fading Channels", *IEEE Veh. Tech.*, vol. 40, no. 4, pp. 686-693, Nov. 1991.

[3] M.L. Moher and J.H. Lodge, "TCMP - A Modulation and Coding Strategy for Rician Channels", *J. Sel. Areas Comm.*, vol SAC-7, pp 1347-1355, Dec. 1989.

[4] D. Parsons, *The Mobile Radio Propagation Channel*, New York: Wiley, 1992.

[5] J.G. Proakis, *Digital Communications*, 2nd Ed., New York: MacGraw-Hill, 1989.

[6] A.J. Viterbi, "When not to spread spectrum - a sequel", *IEEE Comm. Mag.*, vol. 23, no. 4, pp. 12-17, April 1985.

[7] D.V. Sarwate and M.B. Pursley, "Crosscorrelation Properties of Pseudorandom and Related Sequences", Proc. IEEE, Vol. 68, pp. 593 - 619, May 1980.

[8] R.S. Mowbray, R.D. Pringle, P.M. Grant, "Increased CDMA system capacity through adaptive cochannel interference regenaration and cancellation", IEE Proceedings-I, vol. 139, pp. 515 - 524, Oct. 1992.

[9] G. E. Bottomley, "Signature Sequence Selection in a CDMA System with Orthogonal Coding", IEEE Tr. on Veh. Tech., vol. 42, pp. 62 - 68, Feb. 1993.

[10] G. D. Boudreau, D.D. Falconer, S.A. Mahmoud, "A Comparison of Trellis Coded Versus Convolutionally Coded Spread-Spectrum Multiple-Access Systems", IEEE Journal Sel. Areas in Comm., Vol. 8, pp. 628 - 639, May 1990.

[11] D. J. Torrieri, "Performance of Direct-Sequence Systems with Long Pseudonoise Sequences", IEEE Journal Sel. Areas in Comm., Vol. 10, pp. 770-781, May 1992.

[12] R.S. Lunayach, "Performance of a Direct-Sequence Spread-Spectrum Systems with Long Period and Short Period Code Sequences", IEEE Trans. on Comm., vol. COM-31, pp.412-419, March 1983.

[13] K.H. Li, L.B. Milstein, "On the Optimum Processing Gain of a Block-Coded

Direct-Sequence Spread-Spectrum System", IEEE Journal Sel. Areas in Comm., Vol. 7, pp. 618-626, May 1989.

[14] S. Faulkner, "Composite Sequences for Rapid Acquisition of Direct-Sequence Spread Spectrum Signals " Ph.D. Thesis, Carleton University, 1992.

[15] M.B. Pursley, "Performance Evaluation of Phase-Coded Spread-Spectrum Multiple-Access Communications I: Systems Analysis", IEEE Trans. on Comm., Vol. 25, pp. 795-799, August 1977.

[16] M.B. Pursley, D. V. Sarwate, "Performance Evaluation of Phase-Coded Spread-Spectrum Multiple-Access Communications II: Code Sequence Analysis", IEEE Trans. on Comm., Vol. 25, pp. 800-803, August 1977.

[17] D.V. Sarwate, M.B. Pursley, T. U. Basar, "Partial Correlation Effects in Direct-Sequence Spread-Spectrum Multiple-Access Communication Systems", IEEE Trans. on Comm., Vol. 32, pp. 567 - 573, May 1984.

DATE DUE

17. JUL.	03		
09 DEC	03		
22. JUL.	04.		